Synthesizing Parallel Flexures That Mimic the Kinematics of Serial Flexures Using Freedom and Constraint Topologies

Jonathan B. Hopkins
Lawrence Livermore National Laboratory,
L-223, 7000 East Avenue L-223,
Livermore, CA 94551
e-mail: hopkins30@llnl.gov

The principles of the freedom and constraint topologies (FACT) synthesis approach are adapted and applied to the design of parallel flexure systems that mimic degrees of freedom (DOFs) primarily achievable by serial flexure systems. FACT provides designers with a comprehensive library of geometric shapes. These shapes enable designers to visualize the regions wherein compliant flexure elements may be placed for achieving desired DOFs. By displacing these shapes far from the point of interest of the stage of a flexure system, designers can compare a multiplicity of concepts that utilizes the advantages of both parallel and serial systems. A complete list of which FACT shapes mimic which DOFs when displaced far from the point of interest of the flexure system's stage is provided as well as an intuitive approach for verifying the completeness of this list. The proposed work intends to cater to the design of precision motion stages, optical mounts, microscopy stages, and general purpose flexure bearings. Two case studies are provided to demonstrate the application of the developed procedure. [DOI: 10.1115/1.4024474]

Keywords: parallel and serial flexure systems, Freedom and Constraint Topologies, FACT, screw systems, projective geometry

1 Introduction

Many flexure designers prefer parallel flexure systems to serial systems. Parallel flexure systems (Fig. 1(*a*)) consist of a single rigid stage connected directly to a fixed ground by compliant flexure elements. Serial flexure systems, on the other hand, consist of sequential parallel flexure system constituents stacked together in a chain-like configuration (Fig. 1(*b*)). Parallel flexure systems, due to the presence of a single stage, often possess favorable dynamic characteristics. Thus, parallel flexure systems may typically be designed with higher natural frequencies and driven at higher speeds. Problems inherent to underconstraint may also be avoided with such systems. Serial flexure systems that possess redundant DOFs (Fig. 1(*b*)) are said to be underconstrained [1]. For instance, if the lower stage in Fig. 1(*b*) is held fixed, the stage on top will still be free to translate laterally because both stages possess the same translational DOF. Such underconstrained systems perform poorly in both resonant and quasi-static situations. Serial flexure systems may also suffer from stacked motion errors that accumulate from the individual errors of its parallel constituents.

Although parallel flexure systems are advantageous to serial flexure systems in many ways, some latter systems possess certain DOFs that are not achievable by the former. A stage that possesses only three translational DOFs (XYZ), for instance, may only be achieved by serial/hybrid flexure systems (e.g., Fig. 2(*a*)). Note here that flexure systems that consist of combinations of parallel and serial flexure system constituents (often called hybrid systems) are considered serial systems for the purposes of this paper. A parallel flexure system cannot achieve three XYZ translational DOFs because at least one of these DOFs will always be constrained by flexure elements arranged in parallel. Even if only one wire flexure (the most basic flexure element) is applied in parallel, the system's translational DOF along the wire's axis will be constrained (Fig. 2(*b*)). A parallel flexure system's stage can, however, exhibit motions that approximate three translational DOFs if the system's stage is long enough. As an example, consider the system in Fig. 2(*c*). Although this system's blade flexure elements enable its stage to move with two rotational DOFs, R_1 and R_2, and one translational DOF, T_3, the far end of the stage will approximately move with three translational DOFs, T_1, T_2, and T_3, if the stage is long enough. Thus, parallel flexure systems with long stages can mimic the kinematics of serial flexure systems.

The purpose of this paper is to aid the design of long-stage parallel flexure systems that mimic the useful DOFs of serial systems using the principles of the FACT approach [2–4]. In this way, designers can access the advantages of both parallel and serial flexure systems. The FACT synthesis approach utilizes a comprehensive library of geometric shapes that embody the regions of space from which designers can visualize a multiplicity of flexure concepts that achieve desired DOFs. These shapes, which will be discussed in detail in sec. 2, consist of sets of lines that represent directions of constraint or motions along or about their axes. When these shapes are displaced far from the stage's point of interest, as elaborated in this paper, designers can use these shapes to visualize a multiplicity of parallel flexure system concepts that mimic DOFs that are normally only achievable using serial flexure systems. An example of one such FACT shape is the plane shown in Fig. 2(*d*). The blade flexures from this plane represent only one possible flexure topology that could mimic the three translations on the top face of the stage, labeled "Point of Interest." Thus, geometric shapes such as this plane help designers consider many

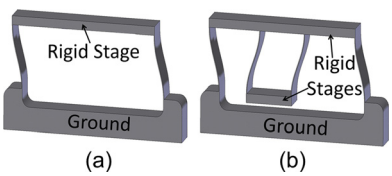

Fig. 1 Parallel (*a*) and serial (*b*) flexure system examples

Contributed by the Mechanisms and Robotics Committee of ASME for publication in the JOURNAL OF MECHANISMS AND ROBOTICS. Manuscript received January 22, 2013; final manuscript received April 29, 2013; published online July 16, 2013. Assoc. Editor: Anupam Saxena.

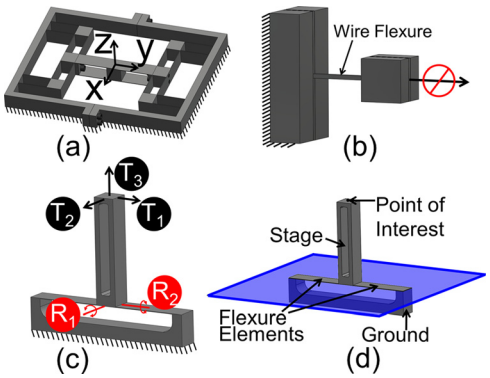

Fig. 2 Three DOF (XYZ) serial flexure system (*a*), wire flexure removes one translation (*b*), parallel flexure that mimics XYZ translations (*c*), and geometric shapes used to synthesize flexure elements (*d*)

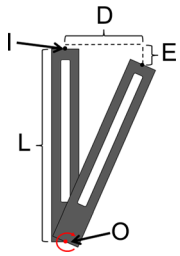

Fig. 3 Parameters for quantifying the approximation errors of parallel flexure systems that mimic the kinematics of serial flexure systems

novel concepts that achieve the desired kinematics before selecting an optimal concept.

The shapes of FACT are visual representations of screw systems [5] that consist of line geometries [6,7] that embody a system's kinematics. Screw systems have traditionally been applied to the design and analysis of spatial mechanisms and robotic manipulators [8–11]. More recently, screw systems have been used in the design of flexures and compliant mechanisms [12–14]. Adding to the significant contributions of Merlet [15] and Hao [16], the FACT methodology presents screw systems as intuitive shapes intended to facilitate efficient synthesis of both parallel and serial flexure systems [17,18].

In this paper, FACT is applied to the design of parallel flexure systems with long stages like the one shown in Fig. 2(*c*) that mimic the kinematics of serial flexure systems. Many of this paper's principles will be explained in the context of this flexure system (Fig. 2(*c*)) because its true and mimicked DOFs are easy to visualize and understand. Although this system may be easily designed, the fundamental principles of FACT are intended to enable designers to synthesize other, more complex, flexure systems, the conception of which may otherwise be difficult.

The specific contributions of this paper are:

(1) An intuitive approach is introduced and coupled with the traditional mathematics of screw theory to generate a comprehensive list of FACT shapes (i.e., screw systems) that mimic the kinematics represented by other FACT shapes when displaced far away in all directions.
(2) A systematic, step-by-step approach is provided to guide designers in using this list of shapes to consider every parallel flexure system concept that mimics the DOFs of serial flexure systems.
(3) Guidelines are established to evaluate how well the parallel flexure systems designed using this approach mimic their intended DOFs.

The long-stage parallel flexure systems of this paper possess unique advantages and challenges. Their measurement errors, for instance, can be minimized by placing the sensors close to the stage's point of interest due to the availability of extra space. The reason for this extra space is that the systems' flexures and actuators are located far from the stage's point of interest. Actuators attached to long-stage parallel flexure system, on the other hand, cannot be isolated without the addition of decoupling flexural elements [19–21]. Moreover, the dynamic characteristics of such systems suffer because their stages are long and bulky and thus cause the system to possess lower natural frequencies. Thus, unnecessary mass should be removed from the stages of these systems without compromising their rigidity. The void at the center of the stage shown in Fig. 2(*d*) was conceived for this reason.

It is important to evaluate how accurately the long-stage parallel flexure systems approximate their intended DOFs. Consider again the system from Fig. 2(*c*), which achieves its intended translation, T_3, but only approximates its translations T_1 and T_2. The accuracy of these translations, which are mimicked by rotations R_1 and R_2, improves with the length of the stage (i.e., the longer the stage, the more accurately these rotations mimic their translations). To quantify this accuracy, consider the parameters defined in Fig. 3. As the stage rotates about point O, the point of interest, I, translates a distance D while simultaneously dipping down a distance E, referred to as the parasitic error. If a designer wished the point of interest to translate over a desired range of $2D$ (the total distance in both directions) while not allowing it to dip below a certain threshold E, the length of the stage, L, will be constrained by the following condition

$$L \geq \frac{D^2 + E^2}{2E} \tag{1}$$

For instance, if a designer desires the system in Fig. 2(*c*) to possess a range of 1 mm ($D = 0.5$ mm) while simultaneously restricting the parasitic error to 1 μm over its full stroke, the length of the stage should be greater than or equal to 12.5 cm. Practical upper limits on the length of the stage also exist based on issues relating to cost, size, and fabrication feasibility, which can be determined by the designer.

The sec. 2 reviews the background principles of FACT. Section 3 describes the novel contributions pertaining to how the shapes of FACT, which represent certain DOFs, may be displaced to mimic other DOFs. Section 4 outlines the process enabling the concepts in Sec. 3 to be utilized for synthesizing parallel flexure systems that mimic the kinematics of serial flexure systems. Two parallel flexure systems are synthesized as case studies using this process.

2 Background Principles

We first review the mathematics necessary to model general DOFs so that we can later synthesize parallel flexure systems that mimic the DOFs of serial flexure systems. All DOFs can be modeled as 6 x 1 vectors called twists [5]. A twist can be visualized as a line about or along which a stage may rotate and/or translate. The pitch of a twist is defined as the ratio of the distance a stage translates along the twist's axis to the coupled rotation about this axis. A general displacement twist, $\mathbf{T}$, is defined as

$$\mathbf{T} = [\,\boldsymbol{\Delta\theta} \quad \boldsymbol{\Delta\delta}\,]^T = [\,\boldsymbol{\Delta\theta} \quad ((\mathbf{c} \times \boldsymbol{\Delta\theta}) + p \cdot \boldsymbol{\Delta\theta}\,)]^T \tag{2}$$

where $\boldsymbol{\Delta\Theta}$ is a 1×3 vector that points along the twist's axis. The magnitude of $\boldsymbol{\Delta\Theta}$ represents the angle through which the stage rotates. The 1×3 vector, $\boldsymbol{\Delta\delta}$, is the linear displacement of the origin of the chosen coordinate system. The location vector, $\mathbf{c}$, is a 1×3 vector that points to any point along the twist's axis from the origin. The twist's pitch is p. These twist parameters are depicted in Fig. 4(*a*). If the twist's pitch is zero or infinite, the twist describes a purely rotational or translational motion,

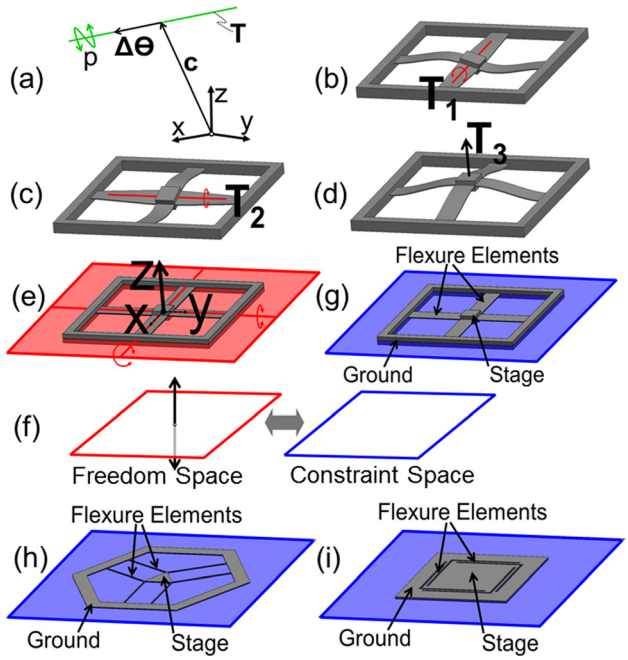

Fig. 4 Twist parameters defined (*a*), DOFs of a parallel flexure system (*b*), (*c*), (*d*), freedom space (*e*), complementary shapes (*f*), constraint space (*g*), and other flexure concepts (*h*), (*i*)

respectively. Otherwise, the twist describes a screw motion. In this paper rotations are depicted as red lines, translations are depicted as black arrows, and screws are depicted as green lines.

Consider the 3-DOF system constrained by four flexure blades shown in Fig. 4. The parallel flexure configuration possesses two rotational DOFs, $\mathbf{T_1}$ and $\mathbf{T_2}$, shown in Figs. 4(*b*) and 4(*c*) and a single translational DOF, $\mathbf{T_3}$, shown in Fig. 4(*d*). If the origin is defined at the center of the stage as shown in Fig. 4(e), a possible location vector, $\mathbf{c}$, for all three twists is a zero vector. The vectors, $\mathbf{\Delta\Theta_1}$ and $\mathbf{\Delta\Theta_2}$, that point along the axes of $\mathbf{T_1}$ and $\mathbf{T_2}$, respectively, are

$$\mathbf{\Delta\theta}_1 = [\,\Delta\theta_1 \quad 0 \quad 0\,] \tag{3}$$

$$\mathbf{\Delta\theta}_2 = [\,0 \quad \Delta\theta_2 \quad 0\,] \tag{4}$$

where $\Delta\Theta_1$ and $\Delta\Theta_2$ are the magnitudes of the two rotational DOFs of the stage. The vector $\mathbf{\Delta\Theta_3}$ that points along the axis of $\mathbf{T_3}$ is a zero vector since it represents a pure translation. Recognizing that the pitches of $\mathbf{T_1}$ and $\mathbf{T_2}$ are zero and that the pitch of $\mathbf{T_3}$ is infinite, these twists may be constructed using Eq. (2) as

$$\mathbf{T_1} = [\,\Delta\theta_1 \quad 0 \quad 0 \quad 0 \quad 0 \quad 0\,]^T \tag{5}$$

$$\mathbf{T_2} = [\,0 \quad \Delta\theta_2 \quad 0 \quad 0 \quad 0 \quad 0\,]^T \tag{6}$$

$$\mathbf{T_3} = [\,0 \quad 0 \quad 0 \quad 0 \quad 0 \quad \Delta\delta_3\,]^T \tag{7}$$

where $\Delta\delta_3$ is the magnitude of the translational DOF of the stage.

Although the three independent twists represent the system's DOFs, they do not represent all permissible motions of the system's stage. If the three DOFs were actuated simultaneously and the relative ratio of their magnitudes was controlled, the stage would rotate about other lines that lie on the surface of the plane shown in Fig. 4(*e*). This plane of rotation lines and the perpendicular translation arrow is the system's freedom space [2–4]. A freedom space is the geometric shape that visually represents the kinematics of a system (i.e., all the twists that the flexure system's constraints permit). The freedom space of a system may be represented mathematically using a single twist vector, $\mathbf{T_{FS}}$, which is the linear combination of the system's DOFs. For the system in Fig. 4, therefore, $\mathbf{T_{FS}}$ may be found using Eqs. (5)–(7) according to

$$\mathbf{T_{FS}} = \mathbf{T_1} + \mathbf{T_2} + \mathbf{T_3} = [\,\Delta\theta_1 \quad \Delta\theta_2 \quad 0 \quad 0 \quad 0 \quad \Delta\delta_3\,]^T \tag{8}$$

where $\Delta\Theta_1$, $\Delta\Theta_2$, and $\Delta\delta_3$ are all independent, real, and finite.

Every parallel flexure system's freedom space uniquely links to a complementary or reciprocal constraint space [2–4] as shown in Fig. 4(*f*). From screw theory, this well-known principle is called duality [8–11,22]. Constraint space is a geometric shape that represents the region from which compliant flexure elements must exist that enable the system's DOFs. The constraint space of the system from Fig. 4 is a plane. This plane is coplanar with the plane of the freedom space. Note that the four flexure blades that connect the system's stage with the ground lie on this constraint space plane as shown in Fig. 4(*g*). All other parallel flexure systems that possess the same three DOFs as this system are expected to be constrained by compliant flexure elements that also lie on a similar constraint space plane. Examples of two such parallel flexure concepts are shown in Figs. 4(*h*) and 4(*i*). Thus, identification of a system's constraint space helps designers visualize various parallel flexure concepts that achieve a desired set of DOFs. This observation is fundamental to the comprehensive nature of the FACT synthesis approach employed in this paper.

All flexure systems can be synthesized using 50 freedom and constraint space pairs, called types in this paper. These types, which are described, derived, and classified in Hopkins [17,18], are shown in Fig. 5. Others have classified similar screw systems in the past for various applications using different criteria. Gibson and Hunt [23,24] introduced a new method for classifying screw systems based on projective geometry. Rico and Duffy [25,26] proposed a comprehensive classification based upon the theory of orthogonal spaces and subspaces [27] by examining the characteristics of the reciprocal basis of screw systems. The geometric shapes in Fig. 5 provide a comprehensive classification of screw systems that enables designers, familiar or not with screw theory, to rapidly visualize and compare parallel and serial flexure system concepts that achieve any desired set of DOFs.

The library in Fig. 5 depicts how the freedom and constraint spaces are organized with an emphasis on the "Parallel Pyramid" (i.e., the pyramid outlined with a thick, black line). The shapes outside of this pyramid represent DOFs that can only be achieved by serial flexure systems. A detailed explanation of this content is provided in Hopkins [18]. Note that all types belong to one of seven columns. Each column pertains to the number of DOFs that the type's freedom space possesses. Within each column, the freedom and constraint space pairs (or types) are numbered. Within the parallel pyramid, the freedom space of each type is shown to the left of a double-sided arrow. The constraint space of the same type is shown to the right of this arrow. Note that the freedom and constraint space pair of the parallel flexure system from Fig. 4(*f*) is type 1 in the 3 DOF column of Fig. 5. The freedom spaces of the types lying outside the parallel pyramid do not link to a complementary constraint space. These are the freedom spaces that represent DOFs that can only be achieved by serial flexure systems. For instance, the freedom space that represents three translational DOFs (XYZ) from the example of Fig. 2(*a*) is among these freedom spaces and is depicted as the sphere of black translation arrows shown as type 20 in the 3 DOF column of Fig. 5. We re-emphasize that (i) the freedom spaces that lie within the parallel pyramid link to constraint spaces that are used to synthesize parallel flexure systems and (ii) the freedom spaces that lie outside of the pyramid do not link to constraint spaces and may thus only be achieved by serial flexure systems that consist of stacked parallel flexure modules. *The goal of this paper is to thus demonstrate how parallel flexure systems may be synthesized using the constraint spaces within the parallel pyramid to mimic the useful kinematics of the freedom spaces that lie outside of the pyramid.* In this way, new parallel flexure systems may be synthesized that possess the advantages of both parallel and serial flexure systems.

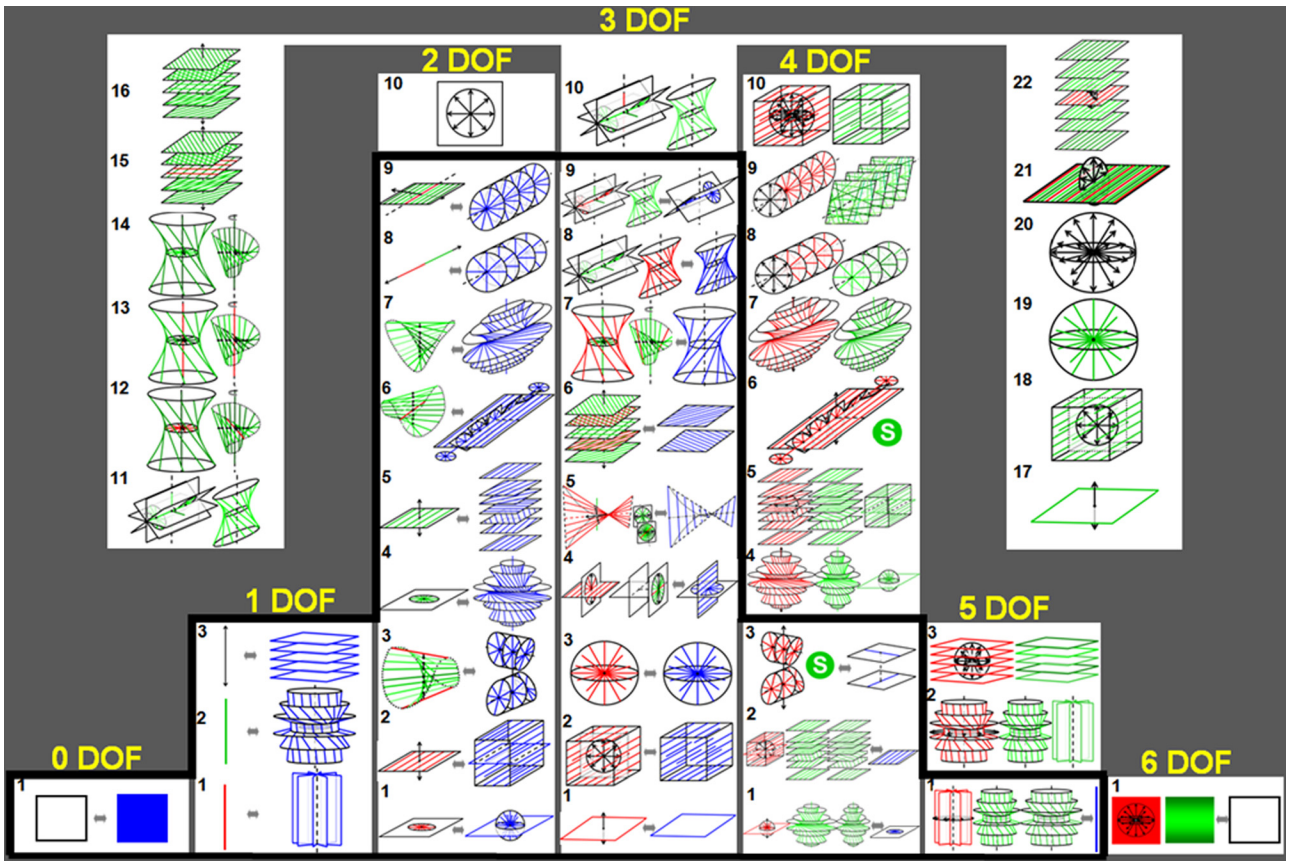

Fig. 5 Comprehensive library of freedom and constraint spaces for flexure synthesis. For details, refer to Ref. [18].

3 Mimicking DOFs by Displacing Freedom Spaces

This section utilizes the principles of projective geometry [28] and screw theory to describe how a freedom space displaced far away may mimic another freedom space. An intuitive, visual approach is developed to predict what freedom spaces will result when other freedom spaces are displaced to infinity. A follow-on logic-based approach is also developed to deduce every freedom space that results from displacing any freedom space to infinity in every direction. Finally key observations that pertain to displacing freedom spaces to infinity are provided.

There are many ways to represent the displacement of a freedom space mathematically. One approach is to apply a transformation matrix [8–11,29,30] to change the reference frame of the freedom space. A transformation matrix, $[N]$, is a 6×6 matrix defined by

$$[N] = \begin{bmatrix} \mathbf{n_1} & \mathbf{n_2} & \mathbf{n_3} & \mathbf{0} & \mathbf{0} & \mathbf{0} \\ \mathbf{L} \times \mathbf{n_1} & \mathbf{L} \times \mathbf{n_2} & \mathbf{L} \times \mathbf{n_3} & \mathbf{n_1} & \mathbf{n_2} & \mathbf{n_3} \end{bmatrix} \tag{9}$$

where $\mathbf{n_1}$, $\mathbf{n_2}$, and $\mathbf{n_3}$ are 3×1 orthogonal unit vectors that represent the axes of the new coordinate reference frame, $\mathbf{0}$ is a 3×1 zero vector, and $\mathbf{L}$ is a 3×1 location vector that points from the origin of the old coordinate system to that of the new reference frame. The twist vector of the freedom space, $\mathbf{T_{FS}}$, may be expressed in the new reference frame as $\mathbf{T'_{FS}}$ according to

$$\mathbf{T'_{FS}} = [N]^{-1}\mathbf{T_{FS}} \tag{10}$$

Consider, for instance, the freedom space of Fig. 4(*e*) shown again in Fig. 6(*a*). According to the coordinate system labeled in the figure, the freedom space's twist vector, $\mathbf{T_{FS}}$, is the same as the vector from Eq. (8). If, however, this twist vector is expressed in a different reference frame with a coordinate system centered in the middle of the stage (Fig. 6(*a*)) with the unit vectors, $\mathbf{n_1}$, $\mathbf{n_2}$, and $\mathbf{n_3}$, along the x', y', and z' axes, respectively, the appropriate transformation matrix $[N]$ is

$$[N] = \begin{bmatrix} [I_{3\times3}] & [0_{3\times3}] \\ \begin{bmatrix} 0 & -d & 0 \\ d & 0 & 0 \\ 0 & 0 & 0 \end{bmatrix} & [I_{3\times3}] \end{bmatrix} \tag{11}$$

where $[I_{3\times3}]$ is a 3×3 identity matrix, $[0_{3\times3}]$ is a 3×3 zero matrix, and d is the magnitude of the location vector $\mathbf{L}$ that points from the old coordinate system to the new coordinate system (i.e., $\mathbf{L} = [0 \;\; 0 \;\; d]$). The freedom space expressed with this new coordinate frame, $\mathbf{T'_{FS}}$, can be calculated by substituting Eqs. (8) and (11) into Eq. (10) as

$$\mathbf{T'_{FS}} = [\,\Delta\theta_1 \quad \Delta\theta_2 \quad 0 \quad \Delta\theta_2 d \quad -\Delta\theta_1 d \quad \Delta\delta_3\,]^T \tag{12}$$

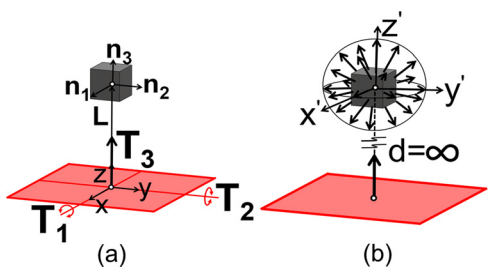

Fig. 6 A planar freedom space of rotation lines and an orthogonal translation (*a*) displaced to infinity in the direction of the translation manifests as a sphere of pure translations (*b*)

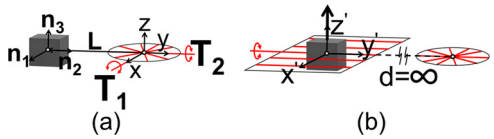

Fig. 7 A disk of rotation lines (*a*) displaced to infinity along one of the axes of its lines manifests as a plane of parallel rotation lines and an orthogonal translation (*b*)

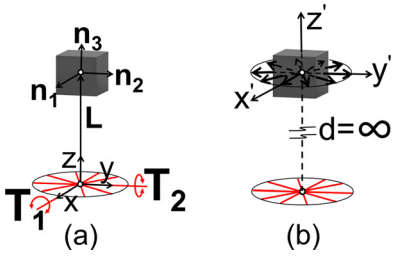

Fig. 8 A disk of rotation lines (*a*) displaced to infinity in a direction perpendicular to its plane manifests as a disk of translation arrows (*b*)

As this freedom space is displaced infinitely far away from the stage such that d approaches infinity, the only way for all the components of the vector from Eq. (12) to remain finite is to allow $\Delta\Theta_1$ and $\Delta\Theta_2$ to approach zero such that

$$\mathbf{T}'_{\mathbf{FS}} = [\,0 \quad 0 \quad 0 \quad \Delta\delta_2 \quad -\Delta\delta_1 \quad \Delta\delta_3\,]^T \tag{13}$$

where $\Delta\delta_2$, $\Delta\delta_1$, and $\Delta\delta_3$ are all independent, real, and finite values (components of any twist must remain finite to represent physically meaningful DOFs). The form of the twist vector in Eq. (13) reveals that the planar freedom space displaced an infinite distance away along the z axis, behaves as a freedom space that represents pure translations in all directions as shown by the sphere of arrows from Fig. 6(*b*). Note from Eqs. (8) and (13) that a positive rotation of $\Delta\Theta_1$ about the x axis manifests itself as a translation along the y' axis in the negative direction (i.e., $-\Delta\delta_1$). Likewise, a positive rotation of $\Delta\Theta_2$ about the y axis manifests as a translation along the x' axis in the positive direction (i.e., $\Delta\delta_2$). Furthermore, a positive translation of $\Delta\delta_3$ along the z axis manifests as the same translation along the z' axis. Intuitively, every other rotation line on the plane of the original freedom space manifests as a single translation within the sphere of the new freedom space. Thus, when the type 1 freedom space from the 3 DOF column of Fig. 5 is displaced to infinity in the direction perpendicular to its plane, the freedom space manifests itself as the type 20 freedom space from the same column.

As another example, consider the freedom space shown in Fig. 7(*a*). This space may be generated by linearly combining two independent twists, $\mathbf{T_1}$ and $\mathbf{T_2}$, as shown. In relation to the coordinate system depicted, the twist vector that describes this entire freedom space, $\mathbf{T_{FS}}$, is given by

$$\mathbf{T_{FS}} = \mathbf{T_1} + \mathbf{T_2} = [\,\Delta\theta_1 \quad \Delta\theta_2 \quad 0 \quad 0 \quad 0 \quad 0\,]^T \tag{14}$$

where $\Delta\Theta_1$ and $\Delta\Theta_2$ represent the independent, real, and finite rotational magnitudes of $\mathbf{T_1}$ and $\mathbf{T_2}$. If we express this freedom space in a different reference frame with its coordinate system centered in the middle of the stage shown in Fig. 7(*a*) with its x', y', and z' axes pointing along the directions of the unit vectors $\mathbf{n_1}$, $\mathbf{n_2}$, and $\mathbf{n_3}$, the transformation matrix $[N]$ is

$$[N] = \begin{bmatrix} [I_{3\times3}] & [0_{3\times3}] \\ \begin{bmatrix} 0 & 0 & -d \\ 0 & 0 & 0 \\ d & 0 & 0 \end{bmatrix} & [I_{3\times3}] \end{bmatrix} \tag{15}$$

where d is the magnitude of the location vector $\mathbf{L}$ that points from the old coordinate system to the new coordinate system (i.e., $\mathbf{L} = [0 \;\; -d \;\; 0]$). The freedom space expressed with this new coordinate frame, $\mathbf{T'_{FS}}$, can be calculated by substituting Eqs. (14) and (15) into Eq. (10) as

$$\mathbf{T}'_{\mathbf{FS}} = [\,\Delta\theta_1 \quad \Delta\theta_2 \quad 0 \quad 0 \quad 0 \quad -\Delta\theta_1 d\,]^T \tag{16}$$

As d approaches infinity (i.e., the freedom space is displaced infinitely far away from the stage), all of the components within the vector from Eq. (16) can be finite only if $\Delta\Theta_1$ approaches zero such that

$$\mathbf{T}'_{\mathbf{FS}} = [\,0 \quad \Delta\theta_2 \quad 0 \quad 0 \quad 0 \quad -\Delta\delta_1\,]^T \tag{17}$$

where $\Delta\theta_2$ and $\Delta\delta_1$ are again independent, real, and finite values. This twist reveals that the disk-like freedom space displaced an infinite distance away along the y axis, behaves as a freedom space that represents every rotation line on a common plane parallel to the line of $\mathbf{T_2}$ and a translation that is orthogonal to that plane as shown in Fig. 7(*b*). Note from Eqs. (16) and (17) that a positive rotation of $\Delta\Theta_1$ about the x axis manifests itself as a translation along the y' axis in the negative direction (i.e., $-\Delta\delta_1$). Furthermore, note that a positive rotation of $\Delta\Theta_2$ about the y axis manifests as the same rotation about the y' axis. The fact that a disk of rotation lines displaced to infinity manifests itself as a plane of parallel rotation lines is expected as, according to projective geometry, all lines that are parallel to one another intersect at the same point at infinity. Thus, when the type 1 freedom space from the 2 DOF column of Fig. 5 is displaced to infinity along any axes of its rotation lines, the freedom space manifests itself as the type 2 freedom space from the same column.

It is important to note that a single freedom space may mimic multiple freedom spaces depending on the direction in which the freedom space is displaced. Consider the freedom space from Fig. 7(*a*) shown in Fig. 8(*a*). When substituting its twist vector from Eq. (14) and the transformation matrix from Eq. (11) into Eq. (10) and allowed the magnitude, d, of vector $\mathbf{L}$ shown in Fig. 8(*a*) to approach infinity, the resulting twist vector is

$$\mathbf{T}'_{\mathbf{FS}} = [\,0 \quad 0 \quad 0 \quad \Delta\delta_2 \quad -\Delta\delta_1 \quad 0\,]^T \tag{18}$$

where $\Delta\delta_2$ and $\Delta\delta_1$ are independent, real, and finite displacement values. This twist reveals that the freedom space displaced an infinite distance away along the z axis, behaves as a freedom space that represents a disk of translation arrows. These arrows point in the same directions as the axes of the rotation lines as shown in Fig. 8(*b*). Note from Eq. (18) that a positive rotation of $\Delta\Theta_1$ about the x axis manifests itself as a translation along the y' axis in the negative direction (i.e., $-\Delta\delta_1$). Furthermore, note that a positive rotation of $\Delta\Theta_2$ about the y axis manifests as a translation along the x' axis in the positive direction (i.e., $\Delta\delta_2$). Thus, the type 1 freedom space from the 2 DOF column of Fig. 5 also manifests itself as the type 10 freedom space from the same column when it is displaced to infinity in a direction perpendicular to the plane of its disk. Note also that this type 10 freedom space lies outside the parallel pyramid of Fig. 5 and may, therefore, only be achieved by stacking parallel modules in series or by using a parallel flexure system like those discussed herein that mimic its kinematics.

It is also important to note that freedom spaces may be displaced to infinity in any direction—not only along the x, y and z axes. Consider the freedom space from Figs. 7(*a*) and 8(*a*) shown again in Fig. 9(*a*). Using the mathematical approach presented here, this disk-like freedom space of rotation lines displaced to infinity along the axis of vector $\mathbf{L}$, manifests itself as another disk of translations as shown in Fig. 9(*b*). This disk of translations is

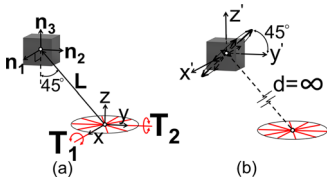

Fig. 9 A disk of rotation lines displaced to infinity in a direction not along the coordinate system's axes (*a*) manifests itself as a disk of translation arrows oriented perpendicular to the direction in which it is displaced (*b*)

oriented differently than it is in Fig. 8(*b*) because of the different direction in which the disk of rotations is displaced. One of the translation arrows of the freedom space points in the [1 0 0] direction and another translation arrow points in the [0 −1 −1] direction in reference to the coordinate system shown in Fig. 9.

Although the freedom space in Fig. 9 did not manifest as a new freedom space when displaced to infinity in an off-axis direction (i.e., the space manifest as another disk of translation arrows similar to Fig. 8), some freedom spaces do manifest as new spaces when they are displaced in directions that are not along their coordinate system axes. An example is the type 7 freedom space from the 3 DOF column of Fig. 5. This freedom space consists of (i) a single set of rotation lines that lie on the surface of a circular hyperboloid centered about the origin of the coordinate system shown in Fig. 10(*a*), (ii) a disk of screws with a common pitch value that lie on the *x*–*y* plane, and (iii) a screw that is coincident with the *z* axis and possesses a pitch value that has an opposite sign to the pitches within the disk. This freedom space also contains other screws (not shown) that lie within cylindroids as described in Hopkins [17]. When this freedom space is displaced along the *x*, *y*, or *z* axes, it will manifest as the type 18 freedom space from the 3 DOF column of Fig. 5 shown in Fig. 10(*b*). This freedom space consists of a disk of translations and a box of screws that are orthogonal to the direction of the translations in the disk. All of these screws have the same pitch value. When, however, the freedom space of Fig. 10(*a*) is displaced to infinity along the direction of any of its rotation lines (i.e., the lines on the surface of the circular hyperboloid), it manifests as the type 2 freedom space from the 3 DOF column of Fig. 5 shown in Fig. 10(*c*). This freedom space is similar to the freedom space of Fig. 10(*b*) except that instead of consisting of parallel screws, it consists of parallel rotation lines.

There are an infinite number of directions along which any given freedom space can be displaced to infinity. However, it is possible to use the analysis in this section to displace any freedom space in finitely many directions to deduce every resulting freedom space and its orientation with respect to the direction of displacement. Recall the three different directions in which the freedom space in Figs. 7(*a*), 8(*a*), and 9(*a*) were displaced. One may deduce from Fig. 7(*b*) that if the freedom space is displaced along the direction of any of its rotation lines—and not just the y axis, it manifests as a plane of rotation lines that are all parallel to

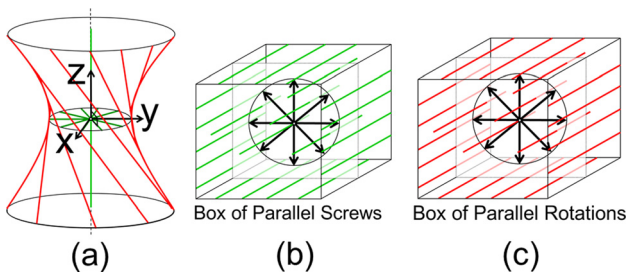

Fig. 10 Type 7 (*a*), type 18 (*b*), and type 2 (*c*) freedom spaces from the 3 DOF column of Fig. 5

the direction along which the disk is displaced, as well as a translation that is orthogonal to this plane. Also, from Figs. 8(*b*) and 9(*b*), if the freedom space is displaced in any other direction, it manifests as a disk of translation arrows, all perpendicular to the direction in which the freedom space is displaced. By considering these few directions of displacement and through intuition and logic, we successfully deduce every freedom space that can manifest by displacing the disk-like freedom space of rotations to infinity in every direction.

Every freedom space from the comprehensive library of Fig. 5 has been displaced in adequate directions to deduce which resulting freedom spaces will manifest and how they will be oriented depending on the direction of displacement. Appendix summaries this information in a comprehensive way that helps designers synthesize parallel flexure systems that mimic the DOFs of serial flexure systems. This Appendix provides a complete list of which freedom spaces manifest as others are displaced to infinity, but it does not contain information on the orientations or the directions in which these other spaces are displaced. To include this information, each of the 50 freedom spaces would require a detailed discussion similar to that on the freedom space in Figs. 7(*a*), 8(*a*), and 9(*a*), which is avoided here for brevity. Sufficient information is, however, provided in Appendix to help designers consider all the freedom space options that could be used to mimic any desired freedom space from the comprehensive library of Fig. 5. It is then up to the designer to apply the procedure in this section to determine the appropriate directions and orientations of these displaced freedom spaces.

The following important observations are noted from the content of Appendix:

(1) Some freedom spaces displaced to infinity in certain directions manifest as themselves. For example, if the freedom space from Figs. 4(*e*) and 6(*a*) was displaced to infinity along the *x* or *y* axes instead of the *z* axis (as labeled), the resulting freedom space would remain unchanged, i.e., it would mimic itself.

(2) Different freedom spaces displaced to infinity can manifest as the same freedom space. For example, the type 17 freedom space from the 3 DOF column of Fig. 5 consists of a translation perpendicular to a plane of screws that share the same pitch value. If this freedom space were displaced infinitely far away from a stage along the axis of its translation, the stage would also behave as the spherical freedom space of pure translations from Fig. 6(*b*). In fact, per Appendix, there are 18 freedom spaces that when displaced to infinity in various directions, manifest as this spherical freedom space of translations (i.e., type 20 from 3 DOF column of Fig. 5).

(3) A freedom space (of *n* DOFs) displaced to infinity from within a particular DOF column in Fig. 5 can only manifest itself as another freedom space that belongs to the same column (*n* DOFs). This observation seems intuitive as DOFs cannot be generated or reduced by merely shifting the position or orientation of a freedom space.

(4) Some freedom spaces represent DOFs that cannot be achieved or mimicked by any parallel flexure system even when freedom spaces are displaced far away. The DOFs of such freedom spaces are exclusively achieved by serial flexure systems. An example is type 6 in the 4 DOF column of Fig. 5. This freedom space lies outside of the parallel pyramid and no freedom space displaced to infinity in any direction will manifest itself as this freedom space.

4 Principles Applied to Flexure Synthesis

The foregoing principles are applied in this section to the design of parallel flexure systems that mimic the DOFs of serial flexure systems. The design process consists of five systematic steps, which are adapted from the original steps of the FACT methodology. Two case studies on the design of parallel flexure

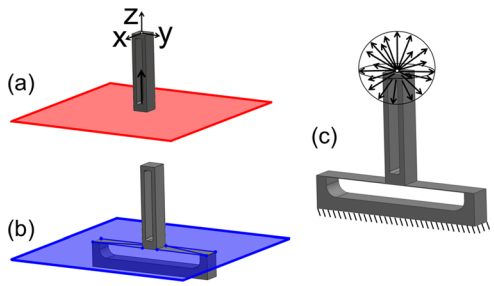

Fig. 11 Freedom space displaced far from the point of interest (*a*), flexure elements selected from the constraint space (*b*), parallel flexure system that mimics XYZ translations (*c*)

systems are presented to demonstrate the application of these steps. For the first study, the flexure system from Fig. 2(*c*) is synthesized.

Step 1: *Identify the parallel flexure system's desired DOFs*. For this case study, the desired DOFs of the parallel flexure system are three orthogonal translations.

Step 2: *Identify the freedom space that represents the desired DOFs from the first step*. This freedom space will result from the linear combination of the DOF twists from step 1. The freedom space that represents the three translations is the sphere of black arrows shown as type 20 in the 3 DOF column of Fig. 5 and in Fig. 6(*b*).

Step 3: *Use the list from Appendix to select and place a freedom space that mimics the freedom space from the second step when displaced far away in a particular direction*. Per Appendix, type 20 in the 3 DOF column from Fig. 5 can be mimicked by displacing types 1, 4, 5, 6, 7, 8, 9, 10, 11, 12, 13, 14, 15, 16, 17, 20, 21, or 22 from the same column to infinity in various directions. The 3 DOF type 1 freedom space is a good selection for this case study. This is because its constraint space is likely to yield an elegant, symmetric, and easily fabricated design. The freedom and constraint spaces of 3 DOF type 1 are shown in Fig. 4(*f*). To mimic the freedom space of 3 DOF type 20, the freedom space of 3 DOF type 1 can be displaced in the direction of its translation as shown in Fig. 6(*b*).

Step 4: *Design a rigid stage long enough to span between its point of interest* (*i.e., the point on the stage intended to approximate the desired DOFs*) *and the freedom space selected and placed from the third step*. The length of this stage should be the distance that the freedom space is displaced in step 3. Equation (1) may be used to quantify how well the final design will approximate the desired DOFs from step 1 for the chosen stage length of this step. For this example, a long rigid stage is designed that connects the point where the stage mimics the three translations to the freedom space of 3 DOF type 1 as shown in Fig. 11(*a*).

Step 5: *Select flexure elements from within the complementary constraint space of the freedom space selected and placed in the third step*. These flexure elements should connect the rigid stage designed in the fourth step to a fixed ground. For more information on how to select the appropriate number and kind of flexure elements from within a constraint space to (i) ensure that the resulting system will only permit the desired DOFs, and (ii) control the system's constraint characteristics (i.e., exact or overconstraint), see Hopkins [2,3,16]. For this example, blade flexures are selected from the plane of the constraint space of 3 DOF type 1 as shown in Fig. 11(*b*).

The final design is depicted in Fig. 11(*c*). For small motions, the top of the stage mimics three translations. The longer the stage, the better these motions mimic pure translations according to Eq. (1). The final design is planar, monolithic and requires no assembly.

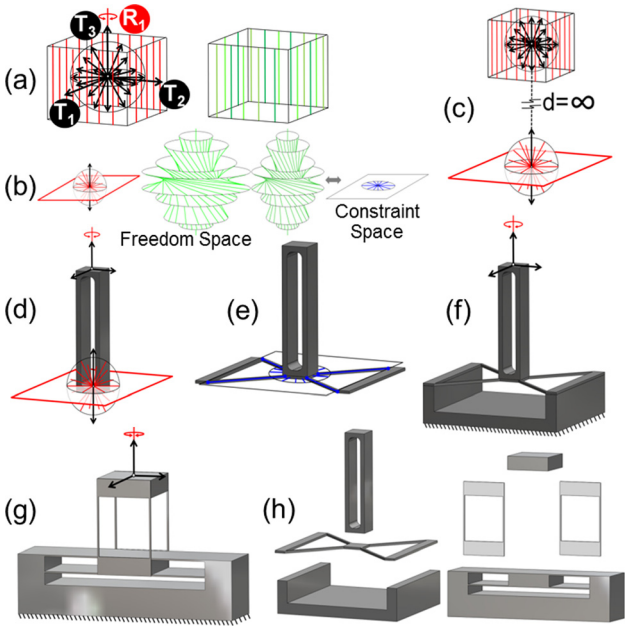

Fig. 12 Freedom space that contains the desired motions (*a*), 4 DOF type 1 freedom and constraint spaces (*b*), approximate freedom space displaced to infinity (*c*), a long stage enables the freedom space to mimic the desired motions (*d*), selecting constraints from the constraint space (*e*), final parallel flexure concept (*f*), serial concept that achieves the same kinematics (*g*), and parts that make up the two concepts (*h*)

4.1 Another Case Study. A second case study further demonstrates the proposed design process. Recall that the first step is to identify the desired DOFs of the parallel flexure system. Here, the intent is to design a stage that possesses four DOFs—three orthogonal translations and a rotation as shown in Fig. 12(*a*).

The second step is to identify the freedom space that represents the desired DOFs from the first step. The freedom space that represents the three translations and the rotation for this example is that of type 10 in the 4 DOF column of Fig. 5. This freedom space consists of a sphere of black translation arrows that point in all directions and a box of infinite extent that contains every red rotation line that is parallel and points in a common direction as shown on the left of Fig. 12(*a*). The freedom space also consists of green screws of all pitch values that are parallel to the rotation lines as shown on the right of the figure. Note that the freedom space shown in Fig. 12(*a*) is oriented differently than the type 10 freedom space shown in the 4 DOF column of Fig. 5. This is because the DOFs selected from the first step must lie within the freedom space from the second step. Note also that this freedom space lies outside the "Parallel Pyramid" and therefore does not possess a constraint space. The desired DOFs in this example may, therefore, be mimicked only by parallel flexure systems of the kind proposed in this paper.

The third step is to use the list from Appendix to choose and place a freedom space that mimics the freedom space from the second step when displaced far away. According to Appendix, type 10 in the 4 DOF column from Fig. 5 can be mimicked by displacing types 1, 2, 3, 4, 5, 6, 7, 8, 9, or 10 from the same column to infinity in various directions. The 4 DOF type 1 freedom space is a proper choice for this example as its constraint space is likely to yield an elegant, symmetric, and easily fabricated design. The freedom and constraint spaces of 4 DOF type 1 are shown in Fig. 12(*b*). Its freedom space, shown on the left side of this figure,

consists of (i) a sphere of red rotation lines that intersect at a common point, (ii) every red rotation line that lies on a plane that passes through this point, (iii) a single black translation arrow that is perpendicular to the plane of rotation lines, and (iv) green screw lines that lie on the surfaces of nested circular hyperboloids. The constraint space of 4 DOF type 1 is a disk of blue constraint lines and is shown on the right of Fig. 12(*b*). To mimic the freedom space of 4 DOF type 10, the freedom space of 4 DOF type 1 can be displaced in the direction shown in Fig. 12(*c*). The red rotation plane mimics the sphere of black arrows, the red sphere of rotation lines mimics the red box of parallel rotation lines and the green circular hyperboloids of screw lines mimic the green box of parallel screw lines.

The fourth step is to design a rigid stage long enough to span between the point of interest that will approximate the desired DOFs and the freedom space selected and placed from the third step. For this example, a long rigid stage is designed such that it connects the point where the stage mimics the four desired DOFs to the freedom space of 4 DOF type 1 as shown in Fig. 12(*d*).

The fifth step is to select compliant flexure elements from within the complementary constraint space of the freedom space selected and placed in the third step. These constraints should connect the rigid stage designed in the fourth step to a fixed ground. For this example, wire flexures are selected from the disk of the constraint space of 4 DOF type 1 as shown in Fig. 12(*e*).

The final design is shown in Fig. 12(*f*). The stage achieves the desired rotational and translational DOFs that are coincident with its axis. The top of the stage mimics the other two translational DOFs that are perpendicular to this axis.

For comparison, a serial version of this parallel flexure system is shown in Fig. 12(*g*). This serial system achieves the same set of DOFs that the parallel system from Fig. 12(*f*) mimics. For finite displacements, however, the serial system will also only mimic the same two translational DOFs because the stage will dip down with a parasitic error along a curved path as the wire flexures deform. Moreover, the rotational DOF will also pull the stage downward with an undesired displacement as it rotates through a finite angle. This rotation induced parasitic error is not an issue for the parallel version of Fig. 12(*f*). FACT can be implemented to design other serial versions that would not possess these parasitic errors, but such designs would tend to be underconstrained, complex, and very difficult to fabricate. Although the serial version in Fig. 12(*g*) is not underconstrained, its two rigid bodies undergo unnecessarily complex dynamics, which can be avoided by using a parallel flexure system. Finally, note that the serial version in Fig. 12(*g*) consists of more parts, which require more fabrication and assemble than the parallel version in Fig. 12(*f*), as shown in Fig. 12(*h*).

Although the parallel design in Fig. 12(*f*) does possess a number of attributes that are advantageous in comparison to the serial design of Fig. 12(*g*), it is not to suggest that the proposed procedure will consistently produce better parallel alternatives to serial designs of similar kinematics. Rather, the intent is to demonstrate that the procedure will consistently provide designers with more concepts to consider and compare during the early stages of design such that the best design may ultimately be selected based on the desired functional requirements.

5 Conclusions

In this paper we adapted the FACT approach such that its principles are used to synthesize parallel flexure systems that mimic the kinematics of serial flexure systems. An intuitive approach is introduced that utilizes screw theory to determine which freedom spaces (i.e., screw systems) can be mimicked by displacing other freedom spaces far from the stage's point of interest in various directions. A complementary systematic approach is also provided that guides designers in using these displaced freedom spaces and their reciprocal constraint spaces to consider every parallel flexure system concept that mimics the DOFs of serial flexure systems. Guidelines are also established to characterize how well such parallel flexure system concepts mimic these DOFs. Two parallel flexure systems are designed as examples to demonstrate the efficacy of this adapted FACT approach.

The main advantage of the approach proposed in this paper is that it is intuitive and requires little to no knowledge of screw theory. Furthermore, the approach is comprehensive in that (i) every geometric shape is determined to synthesize both parallel and serial flexure systems and (ii) the resulting manifestations of every FACT shape are determined when displaced to infinity in every direction. The main limitation is that parallel flexure systems designed using this approach require long stages to accurately mimic the desired kinematics of serial flexure systems. Such bulky stages affect the dynamic characteristics of the system adversely. Work is underway, however, to utilize screw theory to analyze and optimize the dynamic characteristics of such flexure systems [31].

Acknowledgment

This work was performed under the auspices of the U.S. Department of Energy by Lawrence Livermore National Laboratory under Contract No. DE-AC52-07NA27344. LLNL-JRNL-584412.

Appendix: Freedom Spaces That Mimic Other Freedom Spaces at Infinity

This Appendix provides a complete list of freedom spaces that mimic other freedom spaces when displaced to infinity in every direction. The freedom spaces of the types labeled with asterisks represent DOFs that are not achievable by parallel flexure systems directly but may be mimicked by parallel flexure systems using the theory of this paper.

0 DOF Column of Fig. 4

Type 1 is mimicked when type 1 is displaced to infinity.

1 DOF Column of Fig. 4

Type 1 is mimicked when type 1 is displaced to infinity.
Type 2 is mimicked when type 2 is displaced to infinity.
Type 3 is mimicked when types 1, 2, and 3 are displaced to infinity.

2 DOF Column of Fig. 4

Type 1 cannot be mimicked by displacing anything to infinity.
Type 2 is mimicked when types 1, 2, 3, and 6 are displaced to infinity.
Type 3 cannot be mimicked by displacing anything to infinity.
Type 4 cannot be mimicked by displacing anything to infinity.
Type 5 is mimicked when types 3, 4, 5, 6, and 7 are displaced to infinity.
Type 6 cannot be mimicked by displacing anything to infinity.
Type 7 cannot be mimicked by displacing anything to infinity.
Type 8 is mimicked when type 8 is displaced to infinity.
Type 9 is mimicked when type 9 is displaced to infinity.
Type 10* is mimicked when types 1, 2, 3, 4, 5, 6, 7, 8, 9, and 10 are displaced to infinity.

3 DOF Column of Fig. 4

Type 1 is mimicked when type 1 is displaced to infinity.
Type 2 is mimicked when types 2, 3, 4, 7, 8, 9, 10, 12, and 13 are displaced to infinity.
Type 3 cannot be mimicked by displacing anything to infinity.
Type 4 cannot be mimicked by displacing anything to infinity.
Type 5 cannot be mimicked by displacing anything to infinity.
Type 6 is mimicked when types 6 is displaced to infinity.
Type 7 cannot be mimicked by displacing anything to infinity.
Type 8 cannot be mimicked by displacing anything to infinity.
Type 9 cannot be mimicked by displacing anything to infinity.
Type 10 cannot be mimicked by displacing anything to infinity.
Type 11 cannot be mimicked by displacing anything to infinity.

Type 12 cannot be mimicked by displacing anything to infinity.
Type 13 cannot be mimicked by displacing anything to infinity.
Type 14 cannot be mimicked by displacing anything to infinity.
Type 15 is mimicked when type 15 is displaced to infinity.
Type 16 is mimicked when type 16 is displaced to infinity.
Type 17 is mimicked when type 17 is displaced to infinity.
Type 18* is mimicked when types 5, 7, 8, 9, 10, 11, 12, 13, 14, 18, and 19 are displaced to infinity.
Type 19 cannot be mimicked by displacing anything to infinity.
Type 20* is mimicked when types 1, 4, 5, 6, 7, 8, 9, 10, 11, 12, 13, 14, 15, 16, 17, 20, 21 and 22 are displaced to infinity.
Type 21* is mimicked when types 4, 5, and 21 are displaced to infinity.
Type 22* is mimicked when types 4, 5, and 22 are displaced to infinity.

4 DOF Column of Fig. 4

Type 1 cannot be mimicked by displacing anything to infinity.
Type 2 is mimicked when types 1, 2, 3, and 6 are displaced to infinity.
Type 3 cannot be mimicked by displacing anything to infinity.
Type 4 cannot be mimicked by displacing anything to infinity.
Type 5* is mimicked when types 3, 4, 5, 6, and 7 are displaced to infinity.
Type 6 cannot be mimicked by displacing anything to infinity.
Type 7 cannot be mimicked by displacing anything to infinity.
Type 8 is mimicked when type 8 is displaced to infinity.
Type 9 is mimicked when type 9 is displaced to infinity.
Type 10* is mimicked when types 1, 2, 3, 4, 5, 6, 7, 8, 9, and 10 are displaced to infinity.

5 DOF Column of Fig. 4

Type 1 is mimicked when type 1 is displaced to infinity.
Type 2 is mimicked when type 2 is displaced to infinity.
Type 3* is mimicked when types 1, 2, and 3 are displaced to infinity.

6 DOF Column of Fig. 4

Type 1 is mimicked when type 1 is displaced to infinity.

References

[1] Blanding, D. L., 1999, *Exact Constraint: Machine Design Using Kinematic Principles*, ASME Press, New York, NY.
[2] Hopkins, J. B., and Culpepper, M. L., 2010, "Synthesis of Multi-Degree of Freedom, Parallel Flexure System Concepts Via Freedom and Constraint Topology (FACT)—Part I: Principles," Precis. Eng., **34**(2), pp. 259–270.
[3] Hopkins, J. B., and Culpepper, M. L., 2010, "Synthesis of Multi-Degree of Freedom, Parallel Flexure System Concepts Via Freedom and Constraint Topology (FACT)—Part II: Practice," Precis. Eng., **34**(2), pp. 271–278.
[4] Hopkins, J. B., and Culpepper, M. L., 2011, "Synthesis of Precision Serial Flexure Systems Using Freedom and Constraint Topologies (FACT)," Precis. Eng., **35**(4), pp. 638–649.
[5] Ball, R. S., 1900, *A Treatise on the Theory of Screws*, Cambridge University Press, Cambridge, UK.
[6] Merlet, J. P., 2000, *Parallel Robots*, Kluwer Academic Publishers, The Netherlands.
[7] Klein, F., 1921, *Die Allgemeine Lineare Transformation der Linienkoordinaten, Gesammelte math. Abhandlungen I*, Springer, Berlin.
[8] Hunt, K. H., 1978, *Kinematic Geometry of Mechanisms*, Oxford University Press, London.
[9] Phillips, J., 1984, *Freedom in Machinery*, Cambridge University Press, New York, NY.
[10] Murray, R. M., Li, Z., and Sastry, S. S., 1994, *A Mathematical Introduction to Robotic Manipulation*, CRC Press LLC, Boca Raton, FL.
[11] Bothema, R., and Roth, B., 1990, *Theoretical Kinematics*, New York, Dover.
[12] Su, H., Dorozhkin, D. V., and Vance, J. M., 2009, "A Screw Theory Approach for the Conceptual Design of Flexible Joints for Compliant Mechanisms," ASME J. Mech. Rob., **1**(4), p. 041009.
[13] Su, H., and Tari, H., 2010, "Realizing Orthogonal Motions With Wire Flexures Connected in Parallel," ASME J. Mech. Des., **132**(12), p. 121002.
[14] Su, H., and Tari, H., 2011, "On Line Screw Systems and Their Application to Flexure Synthesis," J. Mech. Rob., **3**(1), p. 011009.
[15] Merlet, J. P., 1989 "Singular Configurations of Parallel Manipulators and Grassmann Geometry," Int. J. Rob. Res., **8**(5), pp. 45–56.
[16] Hao, F., and McCarthy, J. M., 1998, "Conditions for Line-Based Singularities in Spatial Platform Manipulators," J. Rob. Syst., **15**(1), pp. 43–55.
[17] Hopkins, J. B., 2007, "Design of Parallel Flexure Systems Via Freedom and Constraint Topologies (FACT)," Masters thesis, Massachusetts Institute of Technology, Cambridge, MA.
[18] Hopkins, J. B., 2010, "Design of Flexure-Based Motion Stages for Mechatronic Systems Via Freedom, Actuation and Constraint Topologies (FACT)," Ph.D. thesis, Massachusetts Institute of Technology, Cambridge, MA.
[19] Awtar, S., and Slocum, A. H., 2007, "Constraint-Based Design of Parallel Kinematic XY Flexure Mechanisms," ASME J. Mech. Des., **129**(8), pp. 816–830.
[20] Li, Y., and Xu., Q., 2009, "Design and Analysis of a Totally Decoupled Flexure-Based XY Parallel Micromanipulator," IEEE Trans. Rob., **25**(3), pp. 645–657.
[21] Li, Y., and Xu, Q., 2011, "A Totally Decoupled Piezo-Driven XYZ Flexure Parallel Micropositioning Stage for Micro/Nanomanipulation," IEEE Trans. Autom. Sci. Eng., **8**(2), pp. 265–279.
[22] Dimentberg, F. M., 1968, *Screw Calculus and Its Applications to Mechanics, Foreign Technology Division*, WP-APB, Ohio.
[23] Gibson, C. G., and Hunt, K. H., 1990, "Geometry of Screw Systems-I, Classification of Screw Systems," Mech. Mach. Theory, **25**(1), pp. 1–10.
[24] Gibson, C. G., and Hunt, K. H., 1990, "Geometry of Screw Systems-II, Classification of Screw Systems," Mech. Mach. Theory, **25**(1), pp. 11–27.
[25] Rico, J. M., and Duffy, J., 1992, "Classification of Screw Systems—I: One- and Two-Systems," Mech. Mach. Theory, **27**(4), pp. 459–470.
[26] Rico, J. M., and Duffy, J., 1992, "Classification of Screw Systems—II: Three-Systems," Mech. Mach. Theory," **27**(4), pp. 471–490.
[27] Rico, J. M., and Duffy, J., 1992, "Orthogonal Spaces and Screw Systems," Mech. Mach. Theory," **27**(4), pp. 451–458.
[28] Coxeter, H. S. M., 1987, *Projective Geometry*, 2nd ed., Springer Press, New York.
[29] Su, H.-J., 2011, "Mobility Analysis of Flexure Mechanisms Via Screw Algebra," ASME J. Mech. Rob. **3**(2), p. 041010.
[30] Hopkins, J. B., and Culpepper, M. L., 2010, "A Screw Theory Basis for Quantitative and Graphical Design Tools That Define Layout of Actuators to Minimize Parasitic Errors in Parallel Flexure Systems," Precis. Eng., **34**(4), pp. 767–776.
[31] Hopkins, J. B., and Panas, R. M., 2013, "Eliminating Parasitic Error in Dynamically Driven Flexure Systems," Proceedings of the 28th Annual Meeting of the American Society for Precision Engineering, St. Paul, MN.